

Article

# Using Molecular Lines to Determine Carbon and Nitrogen Abundances in the Atmospheres of Cool Stars

Tatiana Ryabchikova <sup>1,\*</sup>, Nikolai Piskunov <sup>2</sup> and Yury Pakhomov <sup>1</sup><sup>1</sup> Institute of Astronomy, Russian Academy of Sciences, 119017 Moscow, Russia<sup>2</sup> Department of Physics and Astronomy, Division of Astronomy and Space Physics, Uppsala University, P.O. Box 516, 751 20 Uppsala, Sweden

\* Correspondence: ryabchik@inasan.ru; Tel.: +7-495-951-3980

**Abstract:** Simultaneous analysis of the C<sub>2</sub> and CN molecular bands in the 5100–5200 and 7930–8100 Å spectral regions is a promising alternative for the accurate determination of the carbon (C) and nitrogen (N) abundance in the atmospheres of the solar-like stars. Practical implementation of this new method became possible after recent improvements of the molecular constants for both molecules. The new molecular data predicted the correct line strength and line positions; therefore, they were included in the Vienna Atomic Line Database (VALD), which is widely used by astronomers and spectroscopists. In this paper, we demonstrate that the molecular data analysis provides C and, in particular, N abundances consistent with those derived from the atomic lines. We illustrate this by performing the analysis for three stars. Our results provide strong arguments for using the combination of C<sub>2</sub> and CN molecular lines for accurate nitrogen abundance determination keeping in mind the difficulties of using the N I lines in the observed spectra of the solar-like stars.

**Keywords:** stellar spectra; atomic and molecular data; databases

**Citation:** Ryabchikova, T.; Piskunov, N.; Pakhomov, Y. Using Molecular Lines to Determine Carbon and Nitrogen Abundances in the Atmospheres of Cool Stars. *Atoms* **2022**, *10*, 103. <https://doi.org/10.3390/atoms10040103>

Academic Editor: Emmanouil P. Benis

Received: 5 September 2022

Accepted: 24 September 2022

Published: 27 September 2022

**Publisher's Note:** MDPI stays neutral with regard to jurisdictional claims in published maps and institutional affiliations.



**Copyright:** © 2022 by the authors. Licensee MDPI, Basel, Switzerland. This article is an open access article distributed under the terms and conditions of the Creative Commons Attribution (CC BY) license (<https://creativecommons.org/licenses/by/4.0/>).

## 1. Introduction

The abundances of CNO elements in stellar spectra are extremely important. They reflect many aspects of star formation and stellar evolution. Recent systematic observational and theoretical studies of planet formation have introduced new important aspects of stellar enrichment/depletion of these elements through their inclusion in dust particles (e.g., [1,2]). Differential depletion of certain elements in the accretion flow due to pebble migration in a circumstellar disk and its evolution throughout the lifetime of the disk may and probably does leave a subtle imprint on the relative abundances of the volatile versus refractory elements in stellar atmospheres. The differences between atmospheric abundances of the binary components are very small; therefore, advanced methods for measuring abundances with a precision of 0.03 dex or better are needed. Such methods have been proposed and implemented for carbon and oxygen. They use atomic lines, usually affected by deviations from local thermodynamic equilibrium (NLTE effects) in comparison with abundances derived from diatomic molecules (not subject to strong NLTE effects), such as CH and OH. Such techniques have become possible due to recent advances in atomic and molecular data that proved to be crucial for modeling the NLTE effects in atomic lines and improved the accuracy of the position and strength of individual transitions in molecular bands. For carbon and oxygen, the abundances derived from molecular lines are in excellent agreement with non-LTE analyses of atomic lines. For nitrogen, however, even for the sun, the molecular transitions give a 0.12 dex larger abundance than the atomic lines [3,4]. This is related to the fact that, for solar-like stars, atomic nitrogen has no convenient lines for the analysis comparable to the O I 6156–6158, 7771–7777, 8446 and 9260–9266 Å lines. For example, in the analysis of the nitrogen abundance, Amarsi et al. [5] were only able to use four atomic lines in the 7400–8700 Å and one line in the near infrared region. Moreover, in the spectra of solar-like stars, practically all these lines are blended either with molecular

CN lines or with atomic lines of other elements (see Figure 1), which requires accurate parameters for all contributing lines. Note, that for stars cooler than the sun, it is much more difficult to use N I atomic lines because they become weaker, while the CN blends become stronger. Even the molecular bands of NH are hard to reach as they are mostly located in the UV between 2300 and 3400 Å or in the infrared beyond 1.1 μ, while the spectra obtained for systematic abundance determinations typically cover the range of 3700–9000 Å or at least some parts of it.

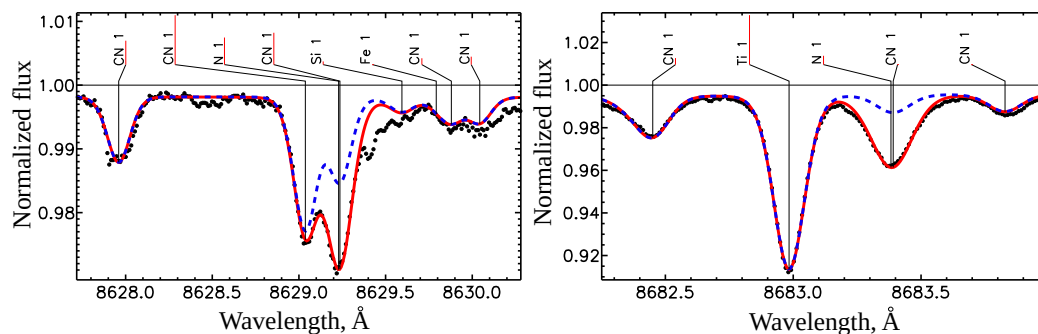


**Figure 1.** Comparison between the Solar Flux Atlas (black dots) and spectrum synthesis in the regions of N I atomic lines (red line). The blue dashed line shows the theoretical calculations without the N I lines demonstrating a blended contribution.

The excellent precision of carbon abundance determination for the sun [6,7] motivated us to try to combine the analysis for C and N by simultaneously interpreting the CN molecular lines around 7950 Å and C<sub>2</sub> lines in 5100–5200 Å (Swan band). In this paper, we present the first results of this analysis. Eventually, the method can be further refined by including the atomic lines of carbon, NLTE, and 3D effects, but we would like to demonstrate its feasibility and also illustrate practical aspects, such as the accessibility of the relevant observations, the availability and the quality of molecular data, and the consistency of the results with other recent determinations.

In the next section we describe our target selection, observational material, and global stellar parameters determination. In Section 3 we present the method and our results, which are then discussed in Section 4.

## 2. Observations and Stellar Atmospheric Parameters

For the analysis, we selected the sun and the wide binary system 16 Cyg with solar-like components. The spectrum of the solar light reflected from asteroid Vesta and spectra of the 16 Cyg components were obtained with the Echelle Spectro Polarimetric Device for Observation of Stars (ESPaDOnS) spectrograph mounted at the 3.6 m Canada–France–Hawaii Telescope ([8], CHFT). The spectral resolving power was  $R = 81\,000$ , and the wavelength coverage was 3696–10,482 Å. All spectra were downloaded from the Canadian Astronomy Data Centre (CADDC) archive [9]. The details of the reduction procedure can be found in [10]. For the sun, we complemented the Vesta spectrum with the Solar Flux Atlas [11], which has much higher spectral resolution and better signal-to-noise ratio (S/N) than the ESPaDOnS observations.

The fundamental stellar parameters (even for the sun), such as effective temperature  $T_{\text{eff}}$ , surface gravity  $\log g$ , metallicity [M/H], projected equatorial rotation ( $v \sin i$ ), micro-turbulent ( $\zeta_t$ ) and macro-turbulent ( $\zeta_{\text{RT}}$ ) velocities as well as the radial velocities were obtained with the help of Spectroscopy Made Easy (SME) software package designed for automatic spectral analysis [12,13]. SME analysis consists of fitting the synthetic spectrum to the observations in chosen spectral regions. The stellar atmospheric parameters are the free parameters of the fit, and a set of weights defines the relative importance of the residuals for each free parameter. When using SME one can select between two approaches: either work with a handful trusted spectral lines or use all the lines that can be reproduced. The first approach was more common in the early days of stellar spectroscopy due to the

patchy quality and poor completeness of atomic and molecular data. The second approach assumes that the distribution of errors in the line data is at least centred on zero and that using many lines will result in correct atmospheric parameters. This assumption is closer to reality for some parameters (e.g.,  $T_{\text{eff}}$ ) and further away for the others (e.g.,  $\log g$ ), but as more and better atomic and molecular data become available through various sources (data producers, compilations, and data centres), the second approach is gaining momentum.

In our analysis, all atomic and molecular line parameters were extracted from VALD [14], which is one of the nodes of the Virtual Atomic and Molecular Data Centre VAMDC [15,16]. The line parameters of NI VALD were collected from the NIST Atomic Spectra Database [17]. Those for the molecular C<sub>2</sub> and CN lines came to VALD from Brooke et al. [18] and Brooke et al. [19], respectively. The line parameters are extracted by the users via VALD extraction tools. In the atmospheres of our target stars, including the sun (Vesta), the atmospheric parameters were determined by Ryabchikova et al. [10] using LLMODELS atmospheric grid [20]. For the solar atlas, we did not perform a fit. Instead, we used the canonical solar 1D atmospheric model computed with the MARCS (Model Atmospheres of Radiative and Convective Stars) code [21]. The atmospheric parameters are presented in Table 1.

**Table 1.** Stellar parameters derived for the sun (Vesta) and in the binary system 16 Cyg using atomic and molecular lines.

Parameter	Sun (Atlas)	Sun (Vesta)	16 Cyg A	16 Cyg B
$T_{\text{eff}}$ , K	5777	5778	5829	5760
$\log g$ , dex	4.44	4.44	4.33	4.39
[M/H]	0.0	0.003	0.110	0.074
$\zeta_t$ , km s <sup>-1</sup>	0.90	0.86	0.99	0.90
$\zeta_{\text{RT}}$ , km s <sup>-1</sup>	3.50	3.59	4.21	3.32

### 3. Carbon and Nitrogen Abundance Determination

Ryabchikova et al. [10] derived the C and N abundances using atomic (C,N) and molecular (C<sub>2</sub>) lines in the atmospheres of the sun (using the Vesta spectrum) and 16 Cyg components. The carbon abundances from the atomic lines were derived from seven lines accounting for departures from the local thermodynamic equilibrium as described by Tsybal et al. [22]. Those from the molecules were derived by using the C<sub>2</sub> molecular lines at 5100–5200 Å (the Swan band), using the conventional SME procedure. The nitrogen abundances were also estimated using two NI  $\lambda\lambda$  8629, 8683 Å lines located in the wing of a strong Ca II line, a member of the IR-triplet, and partially blended with weak molecular CN lines. Carbon and nitrogen abundances are collected in Table 2. Elemental abundances are given as relative values  $\log(N_{\text{el}}/N_{\text{tot}})$ , which corresponds to  $\log \epsilon_{\text{el}} = \log(N_{\text{el}}/N_{\text{tot}}) + 12.04$  in the atmospheres with the solar He abundance. For all stars except the solar atlas, the abundances derived using the atomic lines were taken from Ryabchikova et al. [10]. Carbon and nitrogen solar abundances for the Solar Flux Atlas analysis were determined by the same set of spectral lines employing the same NLTE abundance determination procedure [22] with the NLTE treatment from Alexeeva and Mashonkina [6]. The quality of the NLTE spectrum fitting is illustrated in Figure 1. Note that the carbon abundance derived by using atomic lines based on a 1D static plane-parallel solar model atmosphere, namely  $\log \epsilon_{\text{C}} = 8.44 \pm 0.04$ , exactly matched the state-of-the-art 3D NLTE carbon abundance determinations [7].

Although both NI lines used in our analysis provide consistent abundance results, the abovementioned difficulties in using them for the abundance analysis of a large set of stars require an independent possibility for nitrogen abundance determination. Therefore, we performed simultaneous SME analysis of the C<sub>2</sub> and CN molecular lines in two chosen spectral regions, 5100–5200 Å and 7930–8100 Å. The atmospheric parameters presented in Table 1 were fixed, while the C and N abundances were allowed to vary. Spectral masks in both spectral regions were constructed from numerous unblended and slightly

blended lines of C<sub>2</sub> and CN molecules. We used an SME mask to select 21 intervals in the 5100–5200 Å region and 12 intervals in 7930–8100 Å region for the fitting procedure. An example of such a mask for the solar atlas in the 5100–5200 Å region is shown in Figure 2. The abundance results from the molecular lines are presented in Table 2, while Figure 3 zooms in on small fragments of the selected spectral intervals to allow better comparison between the observed and synthesized spectra of our stars. It is impossible to mark the positions of all individual C<sub>2</sub> lines near the head of the Swan band; therefore, we simply show the synthetic spectra calculated with and without C<sub>2</sub> lines.

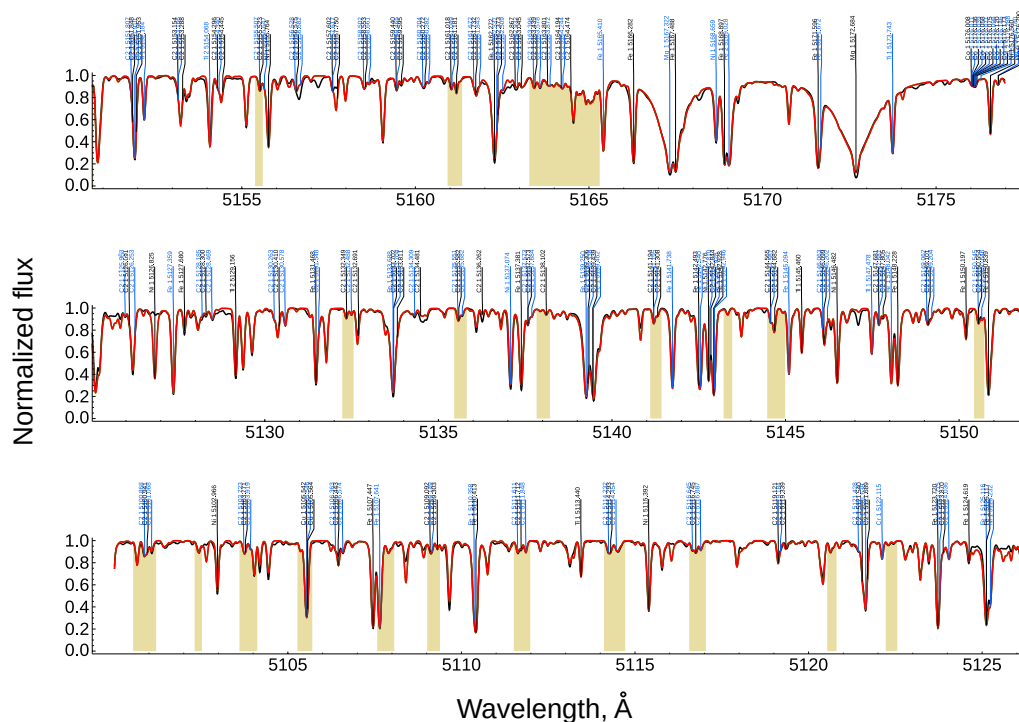


**Figure 2.** Spectral mask in the 5100–5200 Å region of the solar atlas. Observations are shown by the black line. The color bands highlight selected intervals. The SME fitting results are shown by the red line. Only 10% of the strongest transitions are marked on the plot.

The abundance uncertainties given in Table 2 are based on the cumulative distribution analysis performed by SME and tend to be overestimated. In the case of the nitrogen abundance, the statistics (number of points significantly affected by nitrogen abundance) was relatively small in comparison to the carbon (only CN lines versus CN + C<sub>2</sub> lines), and so the core of the distribution is not sufficiently well-defined leading to a less certain estimate. An alternative estimate based on the diagonal of the covariance matrix, which assumes the perfect spectral model generated by SME, gives a similar uncertainty for C abundance and smaller values for N abundance, typically around 0.04 dex for all stars.

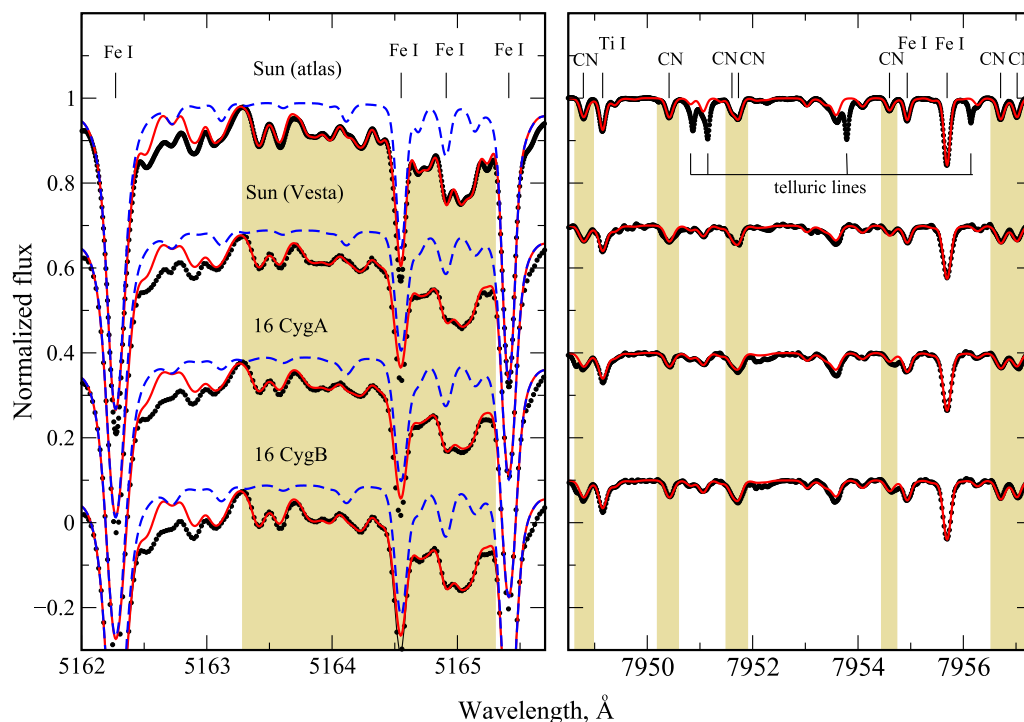


**Figure 3.** Comparison between the observations and spectrum synthesis in the regions of the C<sub>2</sub> Swan bandhead (**left panel**) and CN molecular lines (**right panel**). The observations are shown by black dots, the synthetic spectra calculated with the determined atmospheric parameters and abundances are shown by the solid red line. The fitted intervals are marked by colored bands. The blue dashed lines in the left panel demonstrate theoretical calculations without the C<sub>2</sub> molecular lines.

**Table 2.** Carbon and nitrogen abundances in the sun and in the binary system 16 Cyg derived from the analysis of the atomic and molecular lines.

Species	Sun (Atlas)	Sun (Vesta)	16 Cyg A	16 Cyg B
C (atom)	$-3.596 \pm 0.035$	$-3.601 \pm 0.027$	$-3.560 \pm 0.037$	$-3.564 \pm 0.037$
C (mol)	$-3.600 \pm 0.010$	$-3.617 \pm 0.024$	$-3.564 \pm 0.016$	$-3.571 \pm 0.013$
N (atom)	$-4.089 \pm 0.010$	$-4.062 \pm 0.033$	$-4.063 \pm 0.009$	$-4.076 \pm 0.017$
N (mol)	$-4.072 \pm 0.043$	$-4.059 \pm 0.084$	$-4.006 \pm 0.070$	$-4.038 \pm 0.058$

#### 4. Discussion

We compared the results derived from the 1D LTE (molecules) and NLTE (atoms) analysis of the Solar Flux Atlas with the advocated solar abundances recently published by Asplund et al. [23]. The C and N solar abundances were mostly based on the methods and results presented in Amarsi et al. [4,5,7].

The carbon and nitrogen abundances derived from the atomic and molecular lines agreed well with each other. Our 1D NLTE average carbon abundance  $\log(N_C/N_{\text{tot}}) = -3.60 \pm 0.04$  or  $\log \epsilon_N = 8.44 \pm 0.04$  also agreed with the advocated solar C abundance  $8.46 \pm 0.04$  based on the 3D NLTE analysis of atomic and molecular lines in the solar disk-center intensity spectrum. The resulting nitrogen abundance from the atomic lines was  $\log(N_N/N_{\text{tot}}) = -4.09 \pm 0.01$  or  $\log \epsilon_N = 7.95 \pm 0.01$ . It agreed with the molecular nitrogen abundance derived by Amarsi et al. [4] using the same MARCS solar model, and it was only 0.06 dex higher than their N abundance from the 3D modelling of the molecular lines. The nitrogen abundance derived by using the CN lines was  $\log \epsilon_N = 7.97 \pm 0.04$ . Applying the 3D correction of  $\approx -0.06$  dex from Amarsi et al. [4], we obtained  $\log \epsilon_N = 7.91 \pm 0.04$  for the solar N abundance from molecular lines. The 3D correction for the nitrogen atomic lines was smaller,  $\approx -0.04$  dex [5], and its application resulted in a nitrogen abundance of

$\log \epsilon_N = 7.91 \pm 0.01$ . Our results obtained from the analysis of the Solar Flux spectrum well agreed with the  $\log \epsilon_N = 7.89 \pm 0.04$  derived by Amarsi et al. [4] from the 3D analysis of molecular NH+CN lines in the solar disk-centre intensity spectrum, and it exceeded by 0.14 dex the nitrogen abundance derived by the same group [5] from the atomic lines.

Note that our 'atomic line' N abundance agreed within the error bars with the  $\log \epsilon_N = 7.88$  derived by Caffau et al. [24] in their 3D analysis of the equivalent widths of the NI lines in the solar disk-center intensity spectrum. We have to emphasize that the 3D studies, Caffau et al. [24] and Amarsi et al. [5], of the NI atomic lines were based on the equivalent widths of partially blended lines, while our analysis was based on fitting of the observed line profiles with the blend contribution accounted for when computing the line absorption coefficient.

It is also interesting that while the equivalent widths in Amarsi et al. [5], Caffau et al. [24] were measured using the same observed solar disk-center intensity spectra, they systematically differed from the smaller values reported in Amarsi et al. [5].

## 5. Conclusions

Our simultaneous analysis of the spectral regions with the C<sub>2</sub> and CN molecular lines in solar-like stars, based on the accurate calculations of the molecular line parameters collected in VALD, provided C and N abundances consistent with those derived from the analysis of atomic lines. However, often the atomic NI lines are difficult or even impossible to use in nitrogen abundance determinations; therefore, this task can be solved by the simultaneous analysis of C<sub>2</sub> and CN molecular lines.

**Author Contributions:** T.R. and N.P. performed atomic and molecular line analysis and wrote the main text of the paper; Y.P. prepared the lists of molecular lines for VALD and created the plots. All authors have read and agreed to the published version of the manuscript.

**Funding:** The current research was partially funded by the Ministry of Science and Higher Education of the Russian Federation under the grant 075-15-2020-780 (N13.1902.21.0039) for T.R. and Y.P.

**Data Availability Statement:** The A&M data used in this study are openly available in the VALD database <http://vald.inasan.ru/~vald3/php/vald.php> accessed on 5 September 2022, <http://vald.astro.uu.se/~vald/php/vald.php> accessed on 5 September 2022. The observational and synthetic spectra are available on request from the corresponding author.

**Acknowledgments:** The facilities of the Canadian Astronomy Data Centre operated by the National Research Council of Canada with the support of the Canadian Space Agency were used in the work.

**Conflicts of Interest:** The authors declare no conflict of interest.

## Abbreviations

The following abbreviations are used in this manuscript:

NIST	National Institute of Standards and Technology
VAMDC	Virtual Atomic and Molecular Data Centre
NLTE	non-local thermodynamic equilibrium
LLmodels	Line-by-line opacities model atmospheres

## References

1. Spina, L.; Sharma, P.; Meléndez, J.; Bedell, M.; Casey, A.R.; Carlos, M.; Franciosini, E.; Vallenari, A. Chemical evidence for planetary ingestion in a quarter of Sun-like stars. *Nat. Astron.* **2021**, *5*, 1163–1169. [CrossRef]
2. Kunitomo, M.; Guillot, T. Imprint of planet formation in the deep interior of the Sun. *Astron. Astrophys.* **2021**, *655*, A51.
3. Amarsi, A.M.; Nissen, P.E.; Skúladóttir, Á. Carbon, oxygen, and iron abundances in disk and halo stars. Implications of 3D non-LTE spectral line formation. *Astron. Astrophys.* **2019**, *630*, A104. [CrossRef]
4. Amarsi, A.M.; Grevesse, N.; Asplund, M.; Collet, R. The solar carbon, nitrogen, and oxygen abundances from a 3D LTE analysis of molecular lines. *Astron. Astrophys.* **2021**, *656*, A113. [CrossRef]
5. Amarsi, A.M.; Grevesse, N.; Gruber, J.; Asplund, M.; Barklem, P.S.; Collet, R. The 3D non-LTE solar nitrogen abundance from atomic lines. *Astron. Astrophys.* **2020**, *636*, A120. [CrossRef]

6. Alexeeva, S.A.; Mashonkina, L.I. Carbon abundances of reference late-type stars from 1D analysis of atomic C I and molecular CH lines. *Mon. Not. R. Astron. Soc.* **2015**, *453*, 1619–1631. [[CrossRef](#)]
7. Amarsi, A.M.; Barklem, P.S.; Collet, R.; Grevesse, N.; Asplund, M. 3D non-LTE line formation of neutral carbon in the Sun. *Astron. Astrophys.* **2019**, *624*, A111. [[CrossRef](#)]
8. Donati, J.F. ESPaDOnS: An Echelle SpectroPolarimetric Device for the Observation of Stars at CFHT. In *Solar Polarization*; Trujillo-Bueno, J., Sanchez Almeida, J., Eds.; Astronomical Society of the Pacific Conference Series; Astronomical Society of the Pacific: San Francisco, CA, USA, 2003; Volume 307, p. 41.
9. Crabtree, D.; Durand, D.; Fisher, W.; Gaudet, S.; Hill, N.; Justice, G.; Morris, S.; Woodsworth, A. The Canadian Astronomy Data Centre. In *Astronomical Data Analysis Software and Systems III*; Crabtree, D.R., Hanisch, R.J., Barnes, J., Eds.; Astronomical Society of the Pacific Conference Series; Astronomical Society of the Pacific: San Francisco, CA, USA, 1994; Volume 61, p. 123.
10. Ryabchikova, T.; Pakhomov, Y.; Mashonkina, L.; Sitnova, T. Detailed abundances of the wide pairs of stars with and without planets: The binary systems 16 Cyg and HD 219542. *Mon. Not. R. Astron. Soc.* **2022**, *514*, 4958–4968. [[CrossRef](#)]
11. Kurucz, R.L.; Furenlid, I.; Brault, J.; Testerman, L. *Solar Flux Atlas from 296 to 1300 nm*; National Solar Observatory: Sunspot, NM, USA, 1984.
12. Valenti, J.A.; Piskunov, N. Spectroscopy made easy: A new tool for fitting observations with synthetic spectra. *Astron. Astrophys. Suppl. Ser.* **1996**, *118*, 595–603. [[CrossRef](#)]
13. Piskunov, N.; Valenti, J.A. Spectroscopy Made Easy: Evolution. *Astron. Astrophys.* **2017**, *597*, A16. [[CrossRef](#)]
14. Ryabchikova, T.; Piskunov, N.; Kurucz, R.L.; Stempels, H.C.; Heiter, U.; Pakhomov, Y.; Barklem, P.S. A major upgrade of the VALD database. *Phys. Scr.* **2015**, *90*, 054005. [[CrossRef](#)]
15. Dubernet, M.L.; Antony, B.K.; Ba, Y.A.; Babikov, Y.L.; Bartschat, K.; Boudon, V.; Braams, B.J.; Chung, H.K.; Daniel, F.; Delahaye, F.; et al. The virtual atomic and molecular data centre (VAMDC) consortium. *J. Phys. At. Mol. Phys.* **2016**, *49*, 074003. [[CrossRef](#)]
16. Albert, D.; Antony, B.K.; Ba, Y.A.; Babikov, Y.L.; Bollard, P.; Boudon, V.; Delahaye, F.; Del Zanna, G.; Dimitrijević, M.S.; Drouin, B.J.; et al. A Decade with VAMDC: Results and Ambitions. *Atoms* **2020**, *8*, 76. [[CrossRef](#)]
17. Ralchenko, Y.; Kramida, A.; Reader, J.; NIST ASD Team. NIST Atomic Spectra Database (ver. 4.0.0). Available online: <https://www.nist.gov/pml/atomic-spectra-database> (accessed on 1 September 2010).
18. Brooke, J.S.A.; Bernath, P.F.; Schmidt, T.W.; Bacsikay, G.B. Line strengths and updated molecular constants for the C<sub>2</sub> Swan system. *J. Quant. Spectrosc. Radiat. Transf.* **2013**, *124*, 11–20. [[CrossRef](#)]
19. Brooke, J.S.A.; Ram, R.S.; Western, C.M.; Li, G.; Schwenke, D.W.; Bernath, P.F. Einstein A Coefficients and Oscillator Strengths for the A <sup>2</sup>II-X <sup>2</sup>Σ<sup>+</sup> (Red) and B<sup>2</sup>Σ<sup>+</sup>-X<sup>2</sup>Σ<sup>+</sup> (Violet) Systems and Rovibrational Transitions in the X <sup>2</sup>Σ<sup>+</sup> State of CN. *Astron. Astrophys. J. Suppl. Ser.* **2014**, *210*, 23. [[CrossRef](#)]
20. Shulyak, D.; Tymbal, V.; Ryabchikova, T.; Stütz, C.; Weiss, W.W. Line-by-line opacity stellar model atmospheres. *Astron. Astrophys.* **2004**, *428*, 993–1000. [[CrossRef](#)]
21. Gustafsson, B.; Edvardsson, B.; Eriksson, K.; Jørgensen, U.G.; Nordlund, Å.; Plez, B. A grid of MARCS model atmospheres for late-type stars. I. Methods and general properties. *Astron. Astrophys.* **2008**, *486*, 951–970. [[CrossRef](#)]
22. Tymbal, V.; Ryabchikova, T.; Sitnova, T. Software for NLTE spectrum fitting. In *Physics of Magnetic Stars*; Romanyuk, I.I., Yakunin, I.A., Kudryavtsev, D.O., Eds.; Astronomical Society of the Pacific Conference Series; Astronomical Society of the Pacific: San Francisco, CA, USA, 2019; Volume 518, p. 247.
23. Asplund, M.; Amarsi, A.M.; Grevesse, N. The chemical make-up of the Sun: A 2020 vision. *Astron. Astrophys.* **2021**, *653*, A141, [[CrossRef](#)]
24. Caffau, E.; Maiorca, E.; Bonifacio, P.; Faraggiana, R.; Steffen, M.; Ludwig, H.G.; Kamp, I.; Busso, M. The solar photospheric nitrogen abundance. Analysis of atomic transitions with 3D and 1D model atmospheres. *Astron. Astrophys.* **2009**, *498*, 877–884. [[CrossRef](#)]